Improving Spine Biofidelity of HYBRID-III 6-Year-Old ATD

Jun Wu[1,2], Libo Cao[1], Matthew P. Reed[2], and Jingwen Hu[2]
[1] The State Key Laboratory of Advanced Design and Manufacturing for Vehicle Body（Hunan University）, Changsha 410082, China
[2]University of Michigan Transportation Research Institute, Ann Arbor, MI 48109, USA

ABSTRACT

Because of the lack of pediatric biomechanical data, the Hybrid-III (HIII) child anthropomorphic test devices (ATDs) are essentially scaled from the mid-size male ATD, and are often criticized for its rigid spine comparing to those from children. In this study, possible design modifications for improving the spine biofidelity of the HIII 6-year-old ATD were explored by child cadaver/volunteer test reconstructions and accident reconstructions using computational modeling and optimization techniques. It was found that the translational characteristics of the cervical and lumbar spine in the current child ATD need to be reduced to achieve realistic spine flexibility. It was also found that adding an additional joint at the thoracic spine region with degree of freedom in both flexion/extension and tension can significantly improve the ATD biofidelity in terms of predicting the overall spine curvature and head excursion in frontal crashes.

INTRODUCTION

Anthropomorphic test devices (ATDs) are mechanical surrogates of human used to evaluate the occupant protection provided by various types of restraint systems in new vehicle designs (Mertz 1993). Current child ATDs, especially the Hybrid III (HIII) child ATDs, are widely used in vehicle safety designs (Backaitis et al. 1994). However, due to the paucity of child cadaver test data, the HIII child ATDs are essentially scaled from the HIII midsize-male ATD (Irwin et al. 1997). Given the significant differences in both mechanical properties and anthropometry between adults and children, the scaling method posed many problems in the biofidelity of the current child ATDs. For example, the HIII child ATDs are often criticized for their stiffer spine compared to real children (Ash et al. 2009; Lopez-Valdes et al. 2009), which results in unrealistic crash kinematics and high neck forces and moments that are not representative of true injury potentials (Sherwood et al. 2003). It is evident that more biofidelic ATD spine is urgently needed for enhancing the protection for child occupants.

In this study, a newly developed child ATD model was used to explore possible design modifications for improving the spine biofidelity of current HIII 6 year-old child ATD by

matching several sets of child volunteer test data, pediatric cadaver test data, and motor-vehicle accident data using optimization techniques. The optimized spine design can provide guidance for future modifications of the current child ATDs, and the ATD model developed in this study can be an effective tool for enhancing child protection in Motor-vehicle crashes (MVCs).

METHODS

ATD model

Spine modification. The baseline model used in this study was a HIII 6YO ATD model originally developed by Hu et al. (2011). It incorporated modified ATD pelvis and abdomen designs developed by Klinich et al. (2010) and capable of predicting submarining in frontal crashes. However, no spine modification was made in this model, and there is only one lumbar spine joint in the whole thoracic and lumbar spine region, which is a reflection of the current child ATD design. Therefore, in this study, a joint with six degrees of freedom (DOF) was added in the middle of the thoracic spine to provide more flexibility to the ATD torso. In addition, the rigid body and ellipsoid representing the back of the original thoracic region were divided into two parts to accommodate the additional thoracic spine joint. The original and modified ATD models are shown in Figure 1.

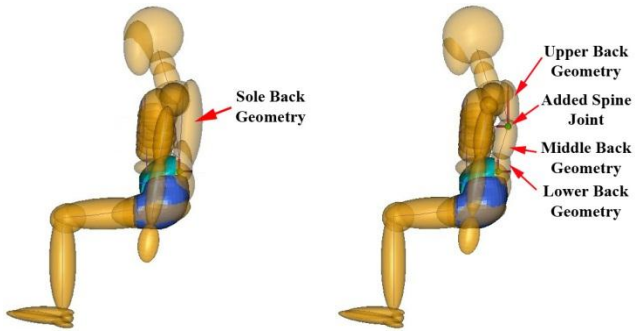

Figure 1: Original (left) and modified (right) thoracic spine model

The translational stiffness and damping coefficient of thoracic spine joint in three directions were initially defined 1×10^5 N/m and 10 Ns/m, respectively, and its rotational stiffness and damping coefficient were initially defined 200 Nm/rad and 100 Nms/rad, respectively. Scaling factors were assigned to the joint characteristics, so that they can be adjusted to match the biomechanical data selected in this study.

ATD model scaling. In this study, to account the variation of age, stature and weight of child subjects in volunteer/cadaver tests and MVCs, a custom software was developed by combining MADYMO Scaler (TASS 2010) and a program written by Scilab V5.2.2 to automatically generate a child ATD model with a target age, weight and height, and at the same time sustaining all modified features (pelvis, abdomen and thoracic spine) on the baseline HIII

6YO ATD model. The MADYMO Scaler manipulated the weight, inertia, joint characteristics, and contact characteristics based on the scaling factors of the ellipsoids in three dimensions, i.e. λx, λy and λz, from the baseline model. Scilab V5.2.2 was used to scale all modified features based on the scaling factors derived from MADYMO Scaler.

Spine range of motion calibration

A child volunteer, whose stature was similar to the HIII 6YO ATD, was tested to provide a reference of spine range of motion (ROM) for the modified ATD model. The child volunteer was seated on a laboratory rigid seat with three postures, namely neutral, slump and flexion, as shown in Figure 2. The spine ROM of the volunteer was qualitatively compared with the physical ATD and ATD model after spine modifications.

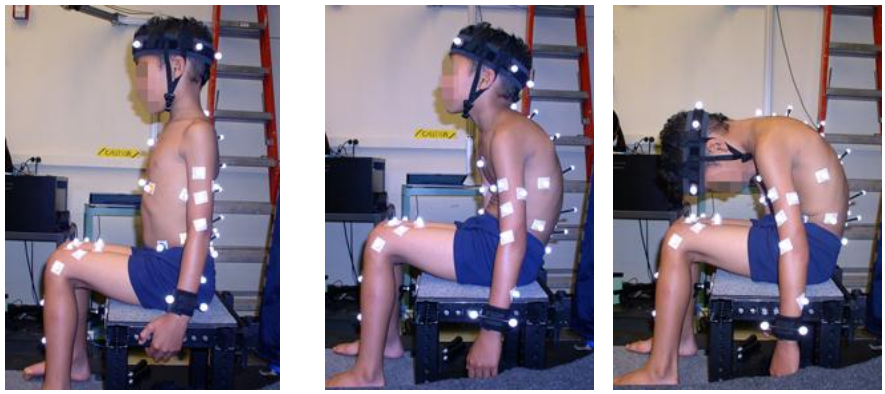

Neutral Slump Flexion

Figure 2: Spine ROM of the child volunteer

Pediatric neck tensile characteristic calibration

In this study, neck tensile response curve for 6YO children developed by Dibb (2011) was used as a reference for child ATD model to match. In the simulations, the ATD head-neck model was set up based on the cadaver tests and human models by Dibb (2011) as shown in Figure 3. The cervical spine was loaded under a velocity of 1 m/s. The neck tensile characteristic of modified ATD model was optimized to match the 6-YO child neck tensile response curve by altering neck joint translational stiffness.

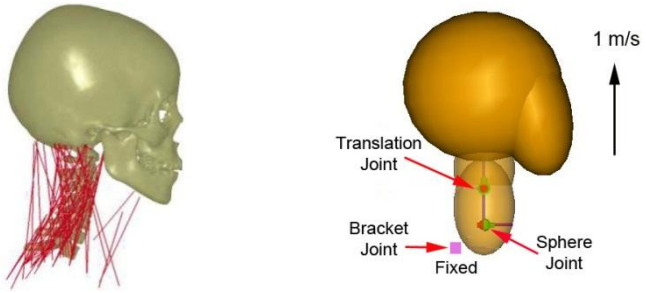

Figure 3: Pediatric neck tensile test (Dibb 2011) and multi-body model setup

Whole-body kinematics calibration

Child volunteer crash tests. Arbogast et al. (2009) conducted a series of pediatric volunteer low-speed crash tests, which is the only pediatric volunteer crash data available in the literature. The crash pulse and test/model setup are shown in Figure 4 and 5. In the tests, markers were attached at head top, opisthocranion, C4, T1, T4, and T8 on each subject. Marker movements in the tests with subjects from 6 to 8 YO were selected in this study, and their average kinematics were used as the target for modified ATD model to match.

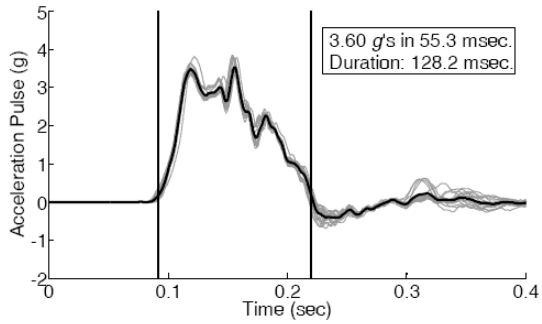

Figure 4: Crash pulse for child volunteer tests (Arbogast et al. 2009)

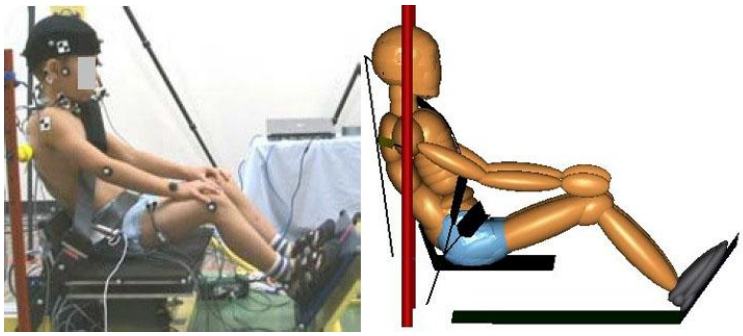

Figure 5: Child volunteer low-speed crash test (Arbogast et al. 2009) and simulation setup

Pediatric cadaver test. Ash (2009) conducted a kinematics comparison between child ATDs and a 13-year old pediatric cadaver in frontal sled tests. The kinematics of the pediatric cadaver was used to calibrate the modified ATD model in this study. The crash pulse and test/model setup are shown in Figure 6 and 7. In the cadaver test, the trajectories of head CG, shoulder, and knee were measured and used as the targets for the computer model to match.

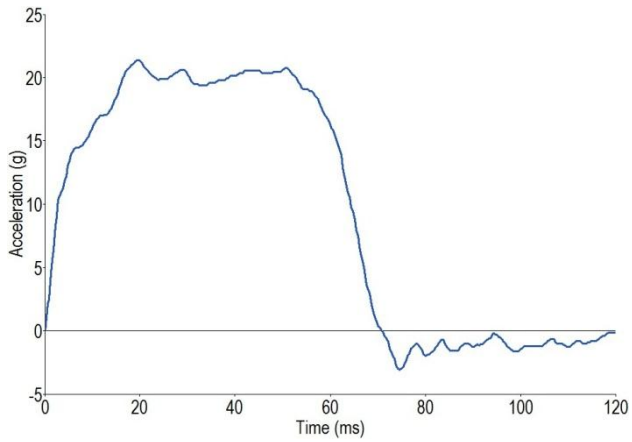

Figure 6: Crash pulse in pediatric cadaver test

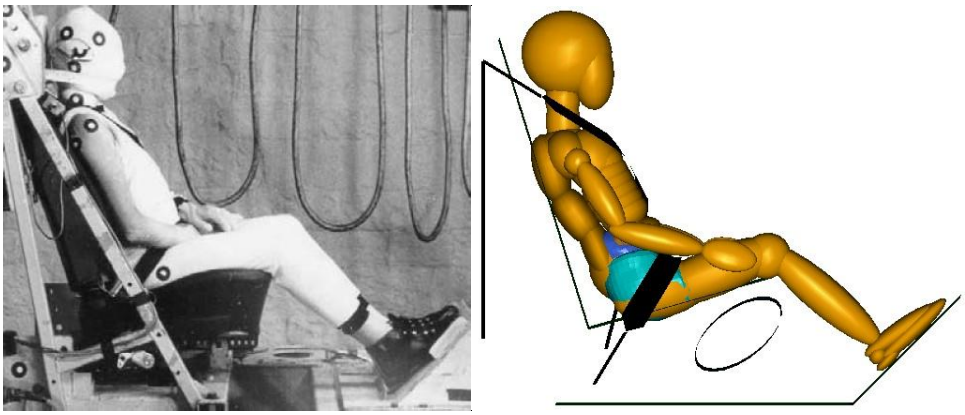
Figure 7: Pediatric cadaver test (Ash et al. 2009) and simulation setup

Due to the difference in anthropometry between the cadaver and the HIII 6YO ATD, the kinematics of cadaver were scaled down for calculating equivalent values corresponding to the HIII 6 YO ATD. The scaling method was based on dimensional analysis from Irwin et al. (1997; 2002), and the length scaling ratio is shown in Equation 1, where λ_L is the scaling factor, L_1 is the seated height of the reference subject and L_2 is the seated height of subject to be scaled. The seated heights and scaling factors of two subjects are shown in Table 1. The scaled kinematics of pediatric cadaver were then used for model calibration.

$$\lambda_L = \frac{L_1}{L_2} \qquad (1)$$

Table 1 : Scale factors and surrogate measurements

	HIII 6 YO	**Pediatric Cadaver**
Seated Height (m)	0.635	0.81
λ_L	1	0.784

MVCs with pediatric head injuries

Two real-world crashes were also selected from the Crash Injury Research and Engineering Network (CIREN) database for ATD model calibration. Two criteria were used for case selection: 1) A 5-10 YO child with head injuries has to be involved, and 2) it has to be a frontal crash with delta V greater than 30 km/h.

Case I (CIREN#33131): A 5 YO boy, 112 cm in height and 23 kg in weight, suffered a severe head injury (AIS4) due to a head contact to the center instrument panel.

Case II (CIREN#551062657): A 6 YO boy, 122 cm in height and 23 kg in weight, suffered AIS1 facial injury due to hitting the panel with his face.

To reconstruct the two accidents, finite element (FE) vehicle models similar to those involved in the accidents were used to estimate the vehicle crash pulse. The vehicle models were setup in the crash conditions provided by the CIREN database, and Ls-Dyna 971 was used as the FE solver. The model-predicted crash pulses are shown in Figure 8, and were input into the MADYMO occupant model. In the occupant model, the vehicle interior was represented by those from available vehicle model with similar interior trim. The restraint systems were defined the same as those in case vehicles, and the child occupant model was generated using the scaling program by controlling age, weight and height. Two occupant models are shown in Figure 9. Head injury criterion (HIC) was the major output from the occupant model for matching the head injury outcomes from the accidents and calibrating the modified ATD spine characteristics. In order to match AIS4 and AIS1 head injuries by HIC values, two head injury risk curves reported by NHTSA (1995) were used to determine the target ranges of the HIC for two selected crashes, as shown in Equation 2 and 3. Head injury risk of 50% was used in this study, leading to a HIC of 358 for the AIS1 head injury and a HIC of 1440 for the AIS4 head injury.

$$\text{AIS1 Injury Risk} = [1 + \exp(1.54 + 200/\text{HIC}) - 0.0065 \times \text{HIC}]^{-1} \quad (2)$$

$$\text{AIS4 Injury Risk} = [1 + \exp(4.9 + 200/\text{HIC}) - 0.00351 \times \text{HIC}]^{-1} \quad (3)$$

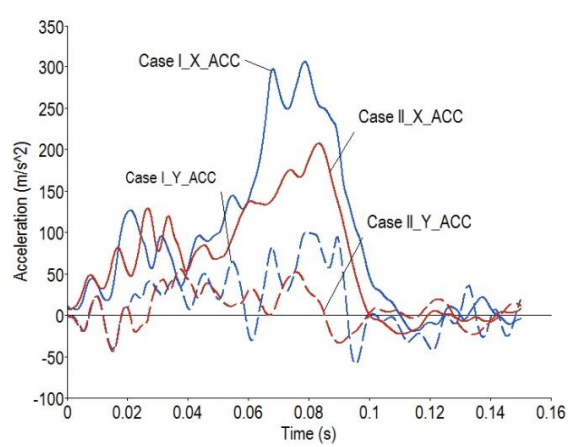

Figure 8: Crash pulse in two cases

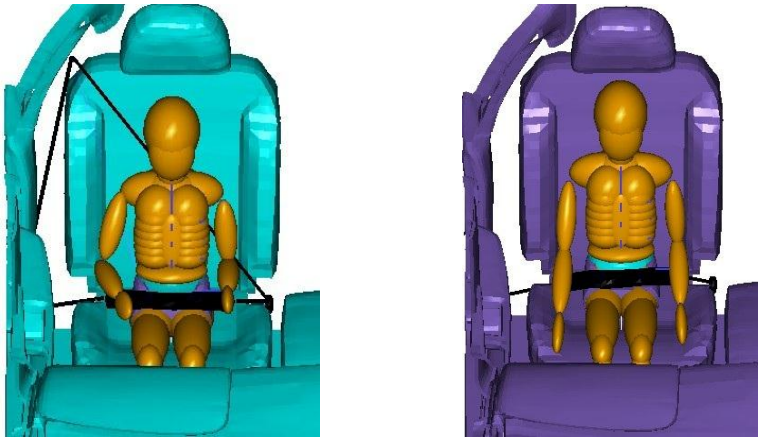

Case I Case II

Figure 9: Model setup for two cases

Normalized error calculation

ATD Model biofidelity was determined by the normalized errors between test and simulation results as shown in Table 2. For neck tensile test, the differences of the referenced tensile response curve and the simulation output was used to calculate the error. For the child volunteer crash test and the pediatric cadaver test, the differences of marker trajectories between the tests and simulations were used to calculate the errors. In the two MVC reconstructions, the differences of simulated and target HIC values were used to calculated the errors.

Table 2: Normalized errors

Crash scenarios	Normalized error calculation
Neck tensile test	$$Error_{Neck} = \frac{\sum_{i=1}^{17}\sqrt{(Sim_i - Reference_i)^2}}{17}$$ Where: i represents the sampling point number on the tensile force-displacement response (1 ms was used as the sampling frequency, and sampling period was 16 ms for both the test and simulation, which resulted in 17 points on tensile force-displacement curve).

Child volunteer crash test		$$Error_{Vol} = \sum_{i=1}^{6} \frac{\sum_{j=1}^{10} \sqrt{\frac{(Sim_{i,j} - Test_{i,j})^2}{Test_{max}^2}}}{10}$$ Where: *i* represents output variable number. 1 to 6 represent normalized sum-of-squares error of head top, opisthocranion, C4, T1, T4, and T8, respectively; *j* represents the sampling point number on the output kinematics. 10 points which equally distribute on the trajectory of markers were extracted for all the tests and simulations.
Pediatric cadaver test		$$Error_{PMHS} = \sum_{i=1}^{4} \frac{\sum_{j=1}^{10} \sqrt{\frac{(Sim_{i,j} - Test_{i,j})^2}{Test_{max}^2}}}{10}$$ Where: *i* represents output variable number. 1 to 4 represent normalized sum-of-squares error of head CG, shoulder, H-point and knee, respectively. *j* represents the sampling point number on the output kinematics. 10 points which equally distribute on the trajectory of markers were extracted for all the tests and simulations.
Motor-vehicle accident reconstructions	Case I	$$Error_{CaseI} = \frac{\lvert Sim - 1440 \rvert}{1440}$$ Where: HIC value 1440 represents AIS4 head injury
	Case II	$$Error_{CaseII} = \frac{\lvert Sim - 358 \rvert}{358}$$ Where: HIC value 358 represents AIS1 head injury

Optimization method

Parameter sensitivity analyses. Parameter sensitivity analyses were conducted for child volunteer crash test, pediatric cadaver crash test and MVCs, to find the most sensitive parameters in determining the ATD model biofidelity, so that fewer parameters can be used for the subsequent optimization to reduce the design space and simulation time. The effect size of each parameter on the normalized errors was used to test the significance level of each parameter.

Model parameters selected for the sensitivity analyses are listed in Table 3. For pediatric cadaver test and child volunteer test, all parameters in Table 3 were included; while for MVCs, knee joint rotational characteristic and chest contact characteristic were excluded because no foot support or shoulder belt was involved. In each sensitivity analysis, Uniform Latin Hypercube sampling method was used to select 600 parameter combinations, and consequently the selected values were uniformly distributed for each parameter.

Table 3: Parameters for sensitivity analysis

Crash Scenarios			Body Region	Input Parameters	Unit	Minimum Bound	Maximum Bound
Pediatric cadaver test	Child volunteer crash test	Two accident reconstructions	Head	Head Mass	%	80%	120%
				Head CG_X	mm	-20	20
				Head CG_Z	mm	-20	20
			Cervical Spine	Translation stiffness	%	10%	1000%
				Rotation stiffness	%	10%	1000%
			Thoracic Spine	Translation stiffness	N/m	1E4	1E6
				Translation damping	Ns/m	0	100
				Rotation stiffness	Nm/rad	100	500
				Rotation damping	Nms /rad	0	300
				Joint_Xpos	mm	-20	20
				Joint_Zpos	mm	-30	30
			Lumbar Spine	Translation stiffness	%	10%	1000%
				Rotation stiffness	%	10%	1000%
			Chest	Contact characteristic	%	10%	1000%
			Knee	Rotation damping	Nms /rad	0	100

Optimization: After parameter sensitivity analysis, the significant factors were chosen as input variables in the process of ATD model calibration. Optimization was used to determine model parameters that provide the best match to the target biomechanical data. ModeFRONTIER 4.3 (ESTECO) was coupled with MADYMO to conduct the optimizations for neck tensile test, child volunteer crash test, pediatric cadaver test, and two MVCs separately in this study. The errors between tests/MVCs and simulations (shown in Table 2) were considered as the objective functions.

In the process of optimization, the baseline ATD model and restraint system were positioned according to the tests/MVCs setup. Simulations were conducted by varying the input variables and the results were then compared to those from the tests or the MVCs. The objective function was minimized by altering parameters of the ATD model until the best match was achieved.

RESULTS

Spine ROM

The spine ROMs of the original HIII 6YO ATD and modified ATD model were compared with those from the volunteer, as shown in Figure 10. The additional thoracic spine joint seemed necessary to provide more realistic spine ROMs than the original ATD. The back curvatures of the original HIII 6YO ATD were fairly straight, and almost the same under three sitting postures. As for the modified ATD model, the additional thoracic spine joint together with the segmented back geometry provided extra flexibility to the spine, making the back curvature more comparable to the child volunteer.

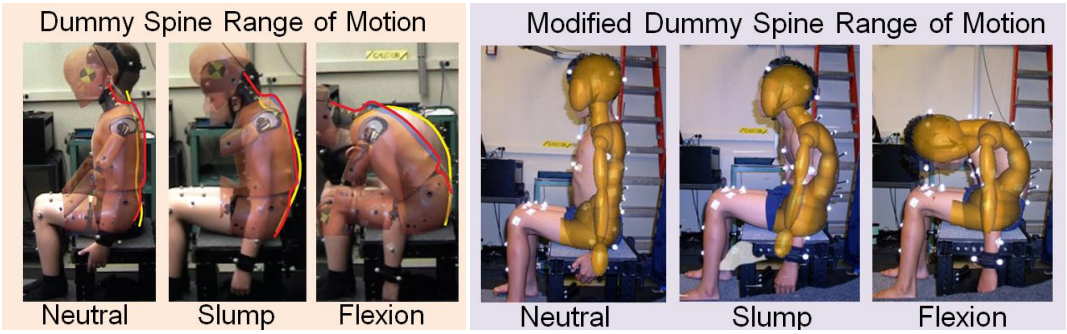

Figure 10: Spine range of motions in original and modified ATD

(Note: The original and modified ATD model were overlaid on the child volunteer in different sitting postures)

Parameter sensitivity analyses

The effect sizes of all parameters on the model errors are showed in Table 4, and the significant parameters was highlighted in bold font. Head mass, rotational stiffness of cervical spine and rotational characteristics (including stiffness and damp) of thoracic spine joint had significant effect in volunteer crash test. Head CG position and the rotational stiffness of cervical spine had a significant effect in pediatric cadaver test. The rotational stiffness of lumbar spine and knee joint characteristic had significant effect in both volunteer crash test and pediatric cadaver test. Head CG position, translational characteristics (including stiffness and damp) of thoracic spine joint, and joint characteristics of cervical and lumbar spine had significant effect in two MVCs.

Table 4: Parameter sensitivity analyses

	Input parameters	**Unit**	**Minimum Bound**	**Maximum Bound**	**Volunteer test**	**Pediatric cadaver test**	**MVCs Case I**	**MVCs Case II**
Head	Head Mass	%	80%	120%	**0.0153**	0.0018	0.9229	0.9541
	Head CG_X	mm	-20	20	0.0015	**0.0025**	0.9732	**0.8746**
	Head CG_Z	mm	-20	20	0.0065	**-0.0021**	**-1.2572**	**-1.1685**
Cervical Spine	Translation stiffness	%	10%	1000%	0.001	-0.0016	**-1.4798**	**-1.5742**
	Rotation stiffness	%	10%	1000%	**-0.1136**	0.0019	-1.081	**-1.2506**
Thoracic Spine	Translation stiffness	N/m	1E5	1E6	-0.0021	0.0004	**-1.5367**	**-1.3586**
	Translation damp	Ns/m	0	100	-0.0039	0.0009	0.9185	**0.8668**
	Rotation stiffness	Nm/rad	100	500	**-0.0162**	**-0.0024**	0.9615	-1.0273
	Rotation damp	Nms /rad	0	300	**-0.0125**	0.0007	0.9903	0.995
	Joint_Xpos	mm	-20	20	0.0026	-0.0009	0.9845	-1.0162
	Joint_Zpos	mm	-30	30	0.005	-0.0007	0.9589	-1.0657
Lumbar Spine	Translation stiffness	%	10%	1000%	-0.0035	0.002	**-1.157**	**-1.1385**
	Rotation stiffness	%	10%	1000%	**-0.0374**	**-0.0232**	**-1.1584**	-1.0545
Chest	Contact characteristic	%	10%	1000%	-0.01	0	-	-
Knee	Rotation damp	Nms /rad	0	20	**0.2547**	**0.0571**	-	-

Note: Bold font indicates significant parameters.

Optimization

Neck tensile test. The optimized neck tensile responses of the 6YO ATD model were compared with the response curves from Dibb (2011) under relaxed and tensed muscle activation states, as shown in Figure 11. The optimized neck tensile response provided much better match than the original response for both relaxed and tensed muscle activation states.

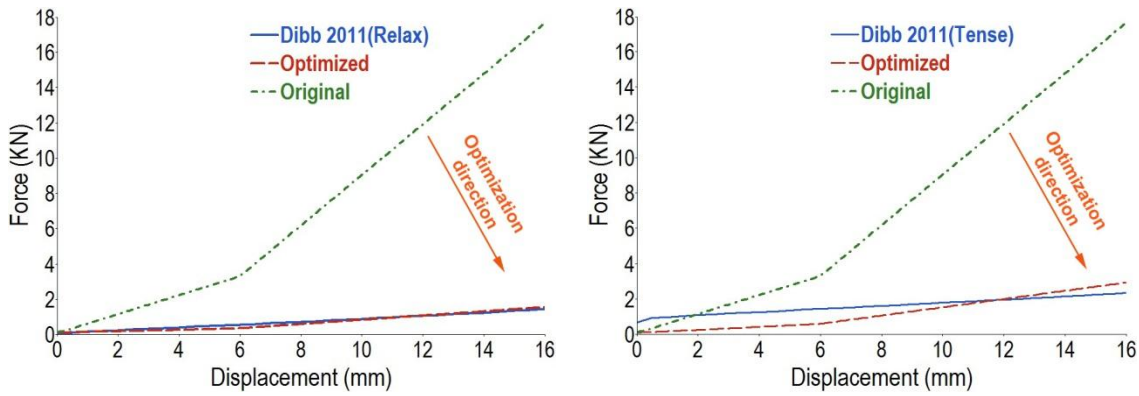

A) Relax B) Tense

Figure 11: Original and optimized neck tensile responses comparing to Dibb (2011) results

Child volunteer crash test. The marker movements from the child volunteer test and simulations were compared before and after optimization, as shown in Figure 12. The optimized marker trajectories were more aligned with the test results than those before optimization. Table 5 quantitatively compared the errors of marker maximal excursions before and after optimization. A significant decrease in the errors at the location of head top, opisthocranion and C4 in x direction was achieved for the modified ATD model.

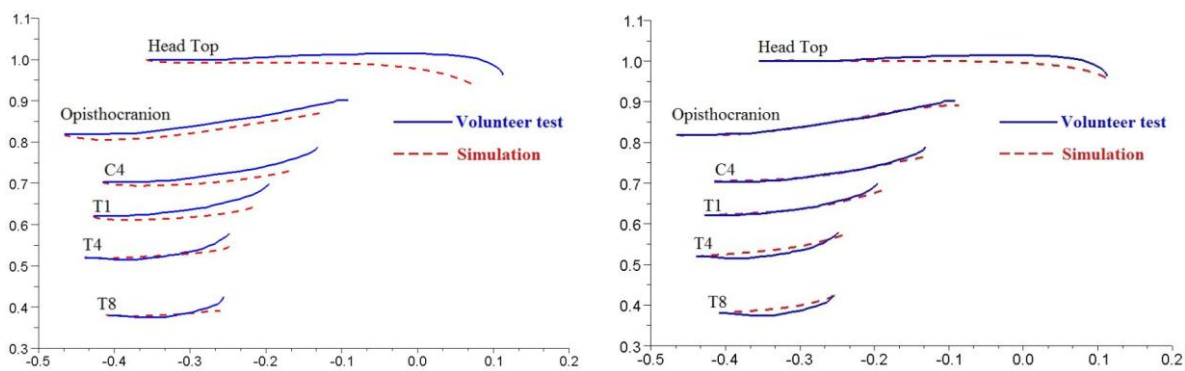

Before optimization After optimization

Figure 12: Comparison of simulated and measured marker movements before and after optimization

Table 5: Kinematic comparison for child volunteer crash test

		Original Model			Improved Model		
Marker		**Simulation**	**Test**	**Error (%)**	**Simulation**	**Test**	**Error (%)**
Head top	x	0.077	0.112	31.4	0.119	0.112	-6.1
	z	0.934	0.967	3.4	0.947	0.967	2.1
Opistho-cranion	x	-0.126	-0.091	-38.4	-0.086	-0.091	5.4
	z	0.872	0.902	3.4	0.892	0.902	1.1
C4	x	-0.161	-0.132	-22	-0.125	-0.132	5.1
	z	0.740	0.789	6.3	0.767	0.789	2.9
T1	x	-0.211	-0.195	-8	-0.186	-0.195	4.7
	z	0.652	0.699	6.8	0.688	0.699	1.6
T4	x	-0.248	-0.248	0	-0.234	-0.248	5.7
	z	0.549	0.579	5.3	0.583	0.579	-0.6
T8	x	-0.261	-0.256	-1.8	-0.252	-0.256	1.7
	z	0.392	0.425	7.9	0.428	0.425	-0.8

Note: data are normalized in x and z by initial z (vertical) position of the subject's head top marker relative the seat pan.

Pediatric cadaver test. The simulated kinematic outputs were compared with the scaled PMHS test results before and after optimization, as shown in Figure 13. Head trajectory predicted by the optimized model was more comparable with the PMHS test results than those from the original model. No significant change was observed on the shoulder or knee movements before and after optimization. The maximal head, shoulder and knee excursions were quantitatively compared before and after optimization, as shown in Table 6. Significant improvement can be found in terms of the head kinematics.

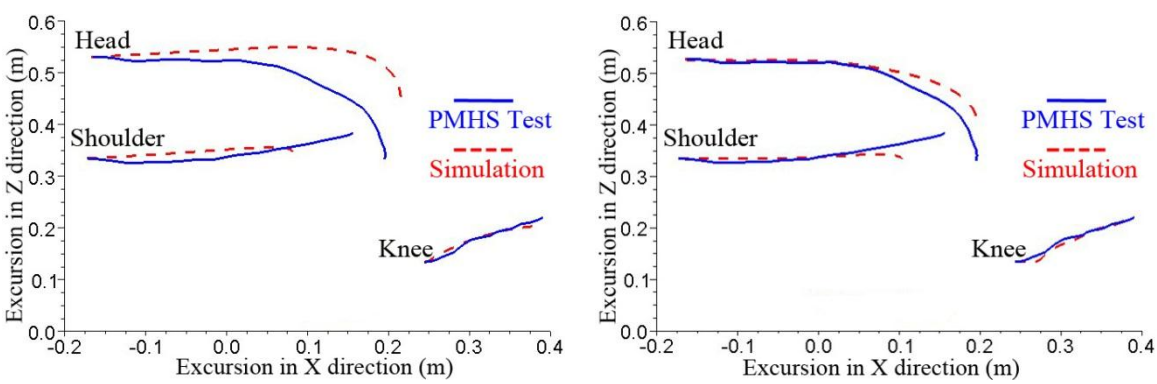

Before optimization After optimization

Figure 13: Comparison of simulated and measured marker movements before and after optimization

Table 6: Kinematic comparison for pediatric cadaver test

		Original Model			Improved Model		
Marker		**Simulation**	**Test**	**Error (%)**	**Simulation**	**Test**	**Error (%)**
Head	x (m)	0.214	0.196	-9.18	0.197	0.196	-0.5
	z (m)	0.445	0.342	-30.12	0.402	0.342	-17.5
Shoulder	x (m)	0.084	0.157	46.5	0.104	0.157	33.76
	z (m)	0.35	0.385	9.09	0.333	0.385	13.51
Knee	x (m)	0.389	0.391	0.51	0.388	0.391	0.77
	z (m)	0.205	0.22	6.82	0.218	0.22	0.91

MVCs. Using the original ATD model without a thoracic spine joint, the stiff spine prevented any head contacts to the instrument panel in both cases. Using the ATD model with an additional thoracic spine joint, as shown in Figure 14, the final optimal model converged to the target HIC values for both cases.

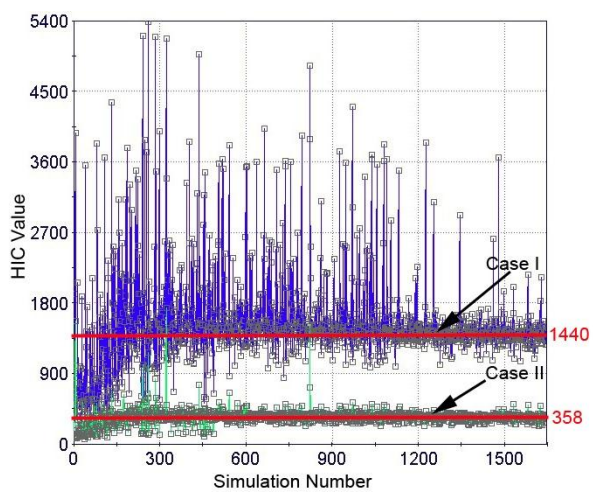

Figure 14: Optimization convergence for two accident reconstructions

Optimized parameter combination. The optimized parameter combinations for all crash conditions are shown in Table 7. All results consistently showed that translational stiffness of cervical spine should be reduced. The results of volunteer test, pediatric cadaver test and two MVCs also indicated that translational stiffness of lumbar spine should be reduced to 0.114 ~ 0.4 of the original value. In addition, the optimal mechanical properties of the added thoracic spine joint were fairly consistent in three crash scenarios. Due to the different restrained status between two MVCs and volunteer/cadaver tests, different rotational stiffness of cervical spine and lumbar were obtained for three crash conditions.

Table 7: Optimized results

	Input parameters	Unit	Neck tensile test		Volunteer test	Pediatric cadaver test	MVCs Case I & II
			Relaxed	Tensed			
Cervical Spine	Translation stiffness	%	0.08	0.16	0.71	0.66	0.17~0.18
	Rotation stiffness	%	-	-	**2.02**	3.96	0.22~0.43
Thoracic Spine	Translation stiffness	N/m	-	-	3.9E5	2.93E5	2.03E5~ 2.08E5
	Translation damp	Ns/m	-	-	53.58	52.4	59~99
	Rotation stiffness	Nm/rad	-	-	**279**	**260**	303~411
	Rotation damp	Nms/rad	-	-	**224.6**	172	76~186
	Joint_Xpos	mm	-	-	9.8	3.8	0.2~11.9
	Joint_Zpos	mm	-	-	7.5	9.4	-0.8~1.2
Lumbar Spine	Translation stiffness	%	-	-	0.4	0.114	0.24~0.28
	Rotation stiffness	%	-	-	**0.89**	**9.24**	0.17~0.21
Knee	Rotation damp	Nms/rad	-	-	**17.6**	**0.77**	-

- Indicate that parameters were not altered in the process of optimization.

DISCUSSION

In order to improve the biofidelity of child ATDs, efforts must be made to use all available sources through innovative approaches. Up to now, the only available child volunteer crash test could be used for calibrating modified child ATD model is low speed frontal impact test conducted at Children's Hospital of Philadelphia (Arbogast et al. 2009). Although the crash pulse in volunteer test was only 3g, it is the only biomechanical test data involved children with the preferred age (6 to 8 YO) and output the whole body kinematics for model to match. Five previous studies compared the impact responses between pediatric cadavers and ATDs (Kallieris et al. 1976; Wismans et al. 1979; Dejeammes et al. 1984; Ash et al. 2009; Seacrist et al. 2010). However, four of these studies involved child seat, which will increase system uncertainty in the process of model validation. In order to simplify the boundary conditions, the test with pediatric cadaver restrained by vehicle seat and seatbelt was adopted in this study to calibrate the modified ATD model (Ash et al. 2009). Accident reconstruction, although limited for its uncertainty, is a good alternative for model validation due to its large sample size and reflection of real crash condition. Therefore, two MVCs with children’s anthropometry similar as HIII 6YO ATD and suffered head injuries were selected in this study for model calibration.

Several previous studies have attempted to improve the child ATD spine biofidelity using simulations. Sherwood et al. (2003) explored the effect of reducing thoracic stiffness on ATD kinematics in crashes by adding a revolution joint at the thoracic spine through MADYMO simulation, and concluded that decreased thoracic spinal stiffness can result in more biofidelic kinematic responses. Ash et al. (2009) used a modified ATD model with a newly added thoracic spine joint to assess the sensitivity of the spine parameters on head excursion for reconstructing a real-world crash. Though both studies reduced thoracic spine stiffness by adding one thoracic spine joint, neither of them calibrates the modified ATD model with any biomechanical test using optimization, nor presented a range of characteristics of the additional thoracic spine joint. In this study, the modified ATD model was optimized using several sets of available test data and accident reconstructions, and the optimal range of joint parameters are valuable for future child ATD modifications.

The ATD kinematics, especially the head excursion, was improved by adding an additional thoracic spine joint. For the volunteer test, the most notable decrease of kinematic error was at the head top, opisthocranion and C4. For pediatric cadaver test, the error of head excursion in the horizontal direction was only 0.5% for the optimized ATD model. The model predicted HIC values in two accident reconstructions were also improved significantly by adding the thoracic spine joint. Modification in cervical and lumbar spine joint also played an important role in the biofidelity of the ATD. Results showed that the cervical spine of the current HIII 6YO ATD is considerably stiffer in tension than children, and should be reduced. This finding is consistent with those from Dibb et al. (2006). The translational stiffness of the lumbar spine joint was also found to be too stiff for the current HIII 6YO ATD. These findings indicated that it is not enough to improve spine biofidelity by just adding rotational DOF, increasing translational DOF to the whole spine is also necessary.

There are two limitations in this study. First, although the MADYMO child ATD model used in this study have been rigorously validated and the pelvis and abdomen regions have been refined by facet meshes, the model is still lack of detailed geometric representation of the physical ATD. Therefore the design modifications presented in this study should be further validated by future tests and investigations. Second, accident reconstructions are limited by the uncertainties in vehicle interior, restraint system, and occupant position and posture, more injury outcomes reflecting the overall occupant kinematics are necessary for improving the accuracy of future accident reconstructions. Nevertheless, this study showed the feasibility of using computational model combined with multiple biomechanical test dataset to improve the ATD biofidelity. The design concepts proposed here may provide valuable information for future child ATD modifications.

CONCLUSIONS

A modified HIII 6YO ATD model was developed and optimized against static child ergonomic data, child volunteer crash test, pediatric cadaver test and two accidents. With the additional thoracic spine joint and optimized joint characteristics in the cervical spine, lumbar spine and knee joints, the modified ATD model provided significantly better biofidelity than the original ATD in terms of the overall spine curvature and head excursion in frontal crashes. It was found that translational stiffness of the cervical and lumbar spine was too high in the current HIII 6YO ATD. Future ATD spine modification should focus on reducing the neck and lumbar tension stiffness, and adding additional flexibility both in flexion/extension and tension at the thoracic spine region. The child ATD model developed in this study can be used as an important tool to improve child ATD biofidelity and child restraint system design in MVCs.

ACKNOWLEDGEMENTS

This research was supported by a Science Fund from the State Key Laboratory of Automotive Safety and Energy in Tsinghua University, Beijing, China.

REFERENCES

Arbogast, K. B., S. Balasubramanian, et al. (2009). "Comparison of kinematic responses of the head and spine for children and adults in low-speed frontal sled tests." Stapp Car Crash Journal **53**: 329-372.

Ash, J., Y. Abdelilah, et al. (2009). Comparison of Anthropomorphic Test Dummies with a Pediatric Cadaver Restrained by a Three-Point Belt in Frontal Sled Tests. Proceedings of the 21st International Technical Conference on the Enhanced Safety of Vehicles (ESV).

Backaitis, S. H. and H. J. Mertz (1994). Hybrid III: The First Human-Like Crash Test Dummy. Society of Automotive Engineers. Warrendale, PA.

Crash Injury Research and Engineering Network, N. H. T. S. A. from Available at: http://www-nass.nhtsa.dot.gov/nass/ciren/SearchForm.aspx.

Dejeammes, M., C. Tarriere, et al. (1984). Exploration of Biomechanical Data Towards a Better Evaluation of Tolerance for Children Involved in Automotive Accidents. Proceedings of the 28th Stapp Car Crash Conference**:** 427-440.

Dibb, A. T. (2011). Pediatric Head and Neck Dynamic Response: A Computational Study.

Dibb, A. T., D. Ottaviano, et al. (2006). Comparative structural neck responses of the THOR-NT, hybrid III, and human in combined tension-bending and pure bending. Stapp Car Crash Conference. **50:** 567-581.

ESTECO (2010). http://www.modefrontier.com/homeMF.html.

Hu, J., K. D. Klinich, et al. (2011). "Development and Validation of a Modified Hybrid-III Six-Year-Old Dummy Model for Simulating Submarining in Motor-Vehicle Crashes." Med Eng Phys **Under review**.

Irwin, A. and H. J. Mertz (1997). Biomechanical Basis for the CRABI and Hybrid III Child Dummies. Proc. 41st Stapp Car Crash Conference, Society of Automotive Engineers, Warrendale, PA.

Irwin, A. L. and H. J. Mertz (1997). Biomechanical bases for the CRABI and Hybrid III child dummies, Society of Automotive Engineers, Warrendale, Pa.

Irwin, A. L., H. J. Mertz, et al. (2002). Guidelines for Assessing the Biofidelity of Side Impact Dummies of Various Sizes and Ages. Society of Automotive Engineers, Warrendale, PA, Copyright © 2002 The Stapp Association. **46:** 297-319.

Kallieris, D., J. Barz, et al. (1976). Comparison between child cadaver and child dummy by using child restraint systems in simulated collisions. Proc. 20th Stapp Car Crash Conference. Society of Automotive Engineers, Warrendale, PA.**:** 511-542.

Lopez-Valdes, F., J. Forman, et al. (2009). "A comparison between a child-size PMHS and the Hybrid III 6YO in a sled frontal impact." Ann Adv Automot Med **53**: 237-246.

Lopez-Valdes, F., J. Forman, et al. (2009). "A comparison between a child-size PMHS and the Hybrid III 6YO in a sled frontal impact." Annals of advances in automotive medicine / Annual Scientific Conference ... Association for the Advancement of Automotive Medicine. Association for the Advancement of Automotive Medicine. Scientific Conference **53**: 237-246.

Mertz, H. J. (1993). Anthropomorphic test devices. Accidental Injury: Biomechanics and prevention, Alan M. Nahum, John Melvin Springer-Verlag, New York**:** 66-84.

NHTSA (1995). "FMVSS No. 201: Upper interior head protection." Final economic assessment.

Seacrist, T., S. Balasubramanian, et al. (2010). "Kinematic Comparison of Pediatric Human Volunteers and the Hybrid III 6-Year-Old Anthropomorphic Test Device." Annals of advances in automotive medicine / Annual Scientific Conference ... Association for the Advancement of Automotive Medicine. Association for the Advancement of Automotive Medicine. Scientific Conference **54**: 97-108.

Sherwood, C. P., C. G. Shaw, et al. (2003). "Prediction of cervical spine injury risk for the 6-year-old child in frontal crashes." Traffic injury prevention **4**(3): 206-213.

TASS (2010). MADYMO Utilities Manual Release 7.2

Wismans, J., J. Maltha, et al. (1979). Child Restraint Evaluation by Experimental and Mathematical Simulation. Proceedings of the 23rd Stapp Car Crash Conference**:** 383-415.